Gondwana accretion tectonics and implications for the geodynamic evolution of eastern Arabia: first structural evidence of the existence of the Cadomian Orogen in Oman (Jabal Akhdar Dome, Central Oman Mountains)

Ivan Callegari[(1)], Andreas Scharf[(2)], Frank Mattern[(2)], Wilfried Bauer[(1)], Andre Jorge Pinto[(1)], Heninjara Rarivoarison[(1)],Katharina Scharf[(1)], Mohammed Al Kindi[(1,3)].

[(1)] GUTech, German University of Technology in Oman, Department of Applied Geosciences, Oman
[(2)] SQU, Sultan Qaboos University, Department of Earth Sciences, Oman
[(3)] Earth Sciences Consultancy Centre, Oman
c.a. ivan.callegari@gutech.edu.om

Abstract

The present work describes two early Cambrian folding events within Cryogenian to earliest Cambrian rocks of the western Jabal Akhdar Dome (Central Oman Mountains). This sequence is truncated at an angular unconformity and topped by Permo-Mesozoic sedimentary shelf strata. The Permo-Mesozoic is brittlely deformed and largely unfolded. This differs in style and intensity of deformation with the refolded underlying Neoproterozoic-Cambrian rocks. Evidences for an older Paleozoic deformation (D1) have been identified within limestone of the Hajir Formation. Tight to close inclined folds (F1) reflect the ductile deformation affecting Neoproterozoic-Cambrian rocks. The folds yield 5-50m amplitudes, with a short-overturned limb, sub-horizontal to gently plunging fold axes and moderately to sub-horizontally inclined axial surfaces. A younger event (D2) has refolded the F1 folds. F2 folds are open to close with amplitudes and wavelengths from several hundred meters to 3 and 5km respectively. The F2 folds display sub-vertical to steep axial planes dipping towards NNW, and fold axes plunging either ENE-wards with ∼50°, or SW-wards with ∼30°, at the northern and southern side of the Jabal Akhdar Dome, respectively.

F2 folds have been mentioned by previous authors as possibly Hercynian in age, while the occurrence of F1 folds is here firstly presented, revealing a uniform NW-vergence of F1 folds after restoration at pre D2 geodynamic conditions.

We present in this work the first structural evidence related to the D1 Cadomian event which occurred in eastern Arabia between ∼542 and 525 ±5Ma, due to the convergence between Arabia and microcontinents and/or oceanic subduction of the Proto-Tethys Ocean. The two deformation events, D1 (Cadomian Orogeny) and D2 (Angudan Orogeny), are related to NE-SW and ∼NW-SE main compressional directions, respectively. The evidence arising from the present research study directly challenges former accounts of a “Hercynian Orogeny” in eastern Arabia.

Keywords

Hajar Mountains; refolded folds; subduction of the Proto-Tethys Ocean; Angudan Orogeny; Gondwana.

Research highlights

- Two early Cambrian compressive events are recorded in the Jabal Akhdar Dome.
- Sigma 1 of the earlier and later events are NE-SW and ∼NW-SE, respectively.
- The earlier and later events are related to the Cadomian and Angudan orogenies.

1. Introduction

The eastern Arabian Plate in the Sultanate of Oman is composed of scarcely exposed but well-represented crystalline basement, representing juvenile Neoproterozoic crust, generated by the collision of volcanic arc terranes between 900 and 750Ma (Mercolli et al., 2006; Whitehouse et al., 2016). This basement is overlain by the Huqf Supergroup, a sequence of weakly metamorphosed sedimentary rocks of Cryogenian to Ediacaran age. In its basal part dominantly glaciogenic sediments were deposited in a rift setting; the upper parts represent siliciclastic and carbonate units of a proximal ramp to shallow marine platform setting (Allen, 2007). The top of the Huqf Supergroup is marked by the volcaniclastic Fara Formation, which is well-exposed in two synclines exclusively in Wadi Bani Awf. Zircon-bearing felsic tuffs and tuffites of this formation yielded U-Pb zircon ages ranging from ~547 to ~542Ma (Brasier et al., 2000; Bowring et al., 2007). The folded Huqf Supergroup is truncated by a Permian unconformity, with a resulting gap in the geological record of the Jebel Akhdar Dome between the early Cambrian and middle Permian.

Paleozoic deformation in the Arabian Plate and the Jabal Akhdar Dome (hereafter JAD) has been described by, e.g., Glennie et al. (1974), Beurrier et al. (1986), Rabu et al. (1986) and Mann and Hanna (1990). This deformation is manifested at the surface by large-scale tight to open folds and reverse/thrust faults, revealing a ~NW/SE-directed compressional phase and the formation of an angular unconformity (e.g., Mann and Hanna, 1990). In the subsurface of Arabia, similarly oriented regional folds and arches have been described, primarly from seismic data (e.g., Faqira et al., 2009; Al-Kindy and Richard, 2014). This deformation has been related to the "Hercynian deformation" (e.g., Glennie et al., 1974; Faqira et al. 2009) or "pre-Permian deformation" (e.g., Mann and Hanna, 1990). Beurrier et al. (1986) and Rabu et al. (1986) relate this deformation to either Late Proterozoic or, more likely, "Hercynian movements". Although the eastern Arabian Plate has been affected by compressional tectonics during the Late Cretaceous and Cenozoic, the pre-Permian rocks have not been folded by those events (see below).

According to the Late Proterozoic-Cambrian palaeogeographic map of Jacobs et al. (2008; their Fig. 1a), the Proto-Tethys Ocean was subducted underneath the northern margin of Gondwana. At that time Arabia formed an integral part of Gondwana with the NW Pakistan Block situated on the seaward side of the Proto-Tethys. Hu et al. (2017; their Fig. 11a) depicted a similar scenario but with two microcontinents involved ("Iran" and "Afghan-NW Pakistan"). These last authors also indicated a subduction age from 557Ma in the NW to 516Ma in the SE. Torsvik and Crocks (2017; their Fig. 5.4), depicted Gondwana for the time slice of 510Ma during which the subduction zone had become inactive in the eastern Arabian segment.

Our goal was to characterize and interpreted the Neoproterozoic to early Cambrian deformation features affecting the oldest rocks in the Jabal Akhdar Dome of the Oman Mountains, therefore elucidating possible deformation events related to the accretionary history of Gondwana. In this framework, we focused on the possible effects of subduction-related convergence to the microcontinents. Furthermore, we want to shed light on the existence of the debated "Hercynian orogenic event" in eastern Arabia (e.g., Glennie et al., 1974), through fold analysis of the relevant formations.

We will present field-based structural evidence for two different early Paleozoic folding events. Following an introduction of the area's geological background and previous published interpretations of Paleozoic deformation in the Oman Mountains, we will present our new findings while discussing their regional importance for the geodynamic understanding of the eastern Arabian Plate. Finally, we will discuss the possible geodynamic origin for these two folding events.

2. Geological and structural setting

The Oman Mountains contain a complex assemblage of thick Neoproterozoic to Neogene siliciclastic and carbonate rocks. The Neoproterozoic and earliest Cambrian rocks (known as the "Autochthonous Unit A"; e.g., Béchennec et al., 1992) are only locally exposed at the cores of two large domes: the Jabal Akhdar and Saih Hatat (SHD) domes (Fig. 1). The Neoproterozoic formations of the Autochthonous Unit A in the Jabal Akhdar area (Fig. 2) are the object of our study. The approached sequence consists of five formations including, from bottom to top, Neoproterozoic Mistal Formation (an alternation of siltstone and sandstone with a diamictite in the lower part, total thickness >1250m), Hajir Formation (100m-thick black fetid limestone), Muaydin Formation (800m of mainly siltstone with thin carbonate beds), Kharus Formation (up to 245m of limestone and dolostone), and Fara Formation (380m chert, volcanoclastics, siltstone, sandstone and conglomerate). The Fara formation corresponds to Neoproterozoic-earliest Cambrian age (Beurrier et al., 1986; Bowring et al., 2007).

SHD's Neoproterozoic formations differ from JAD's, including Hatat and Hiyam Formations (Bauer et al., 2018; Mattern and Scharf, 2019). The latter is overlain by the Cambro-Ordovician Amdeh Formation (Miller et al., 2018) which is not represented in the JAD (Mattern et al., 2018).

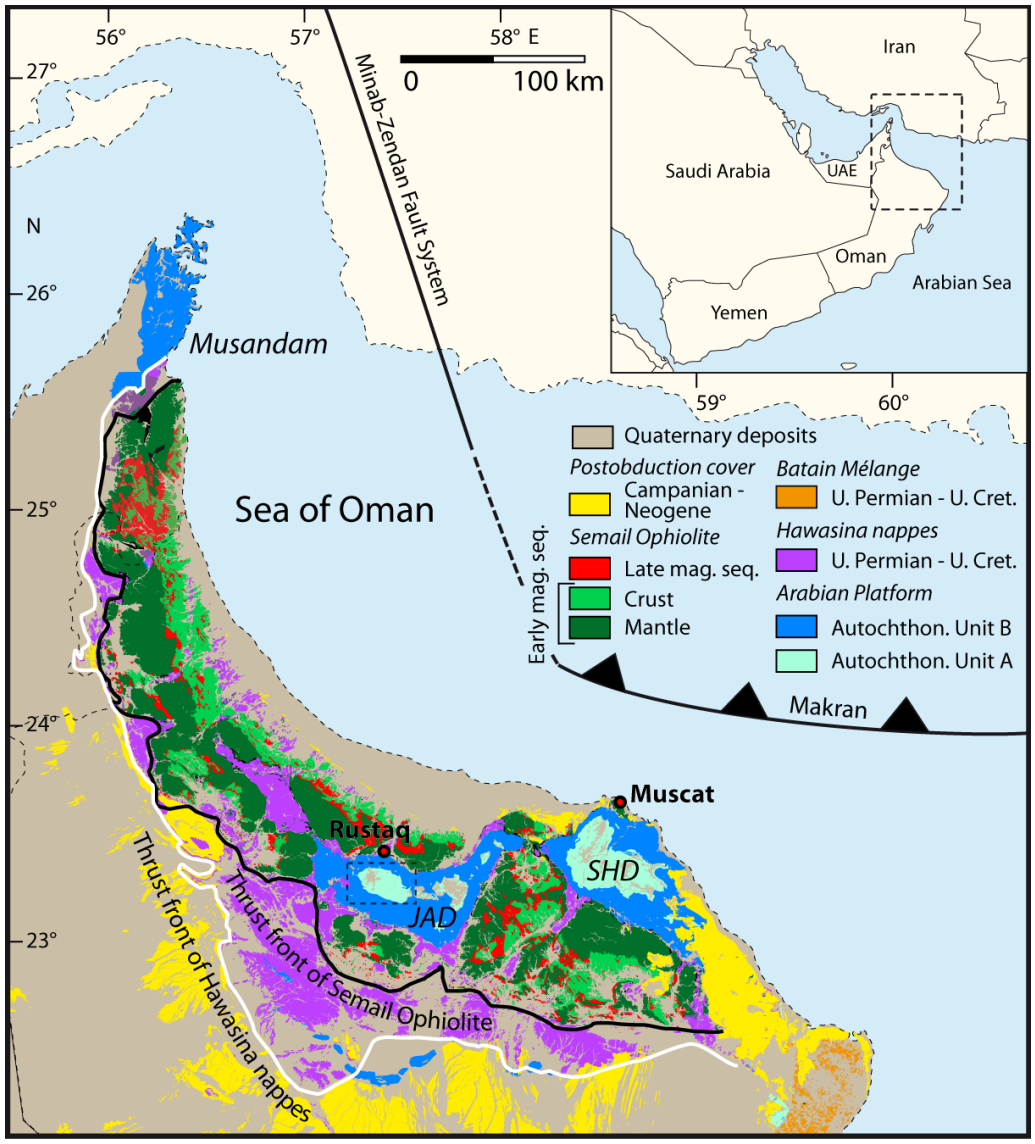

Fig. 1. Tectonic overview map of the northeastern Arabian Peninsula. JAD – Jabal Akhdar Dome; SHD – Saih Hatat Dome. Map modified after Béchennec et al. (1993) and Moraetis et al. (2018). Parts of the northern Oman Mountains are drawn after the geological map from the United Arab Emirates (UAE) (British Geological Survey, 2006). The black dashed rectangle is the study area.

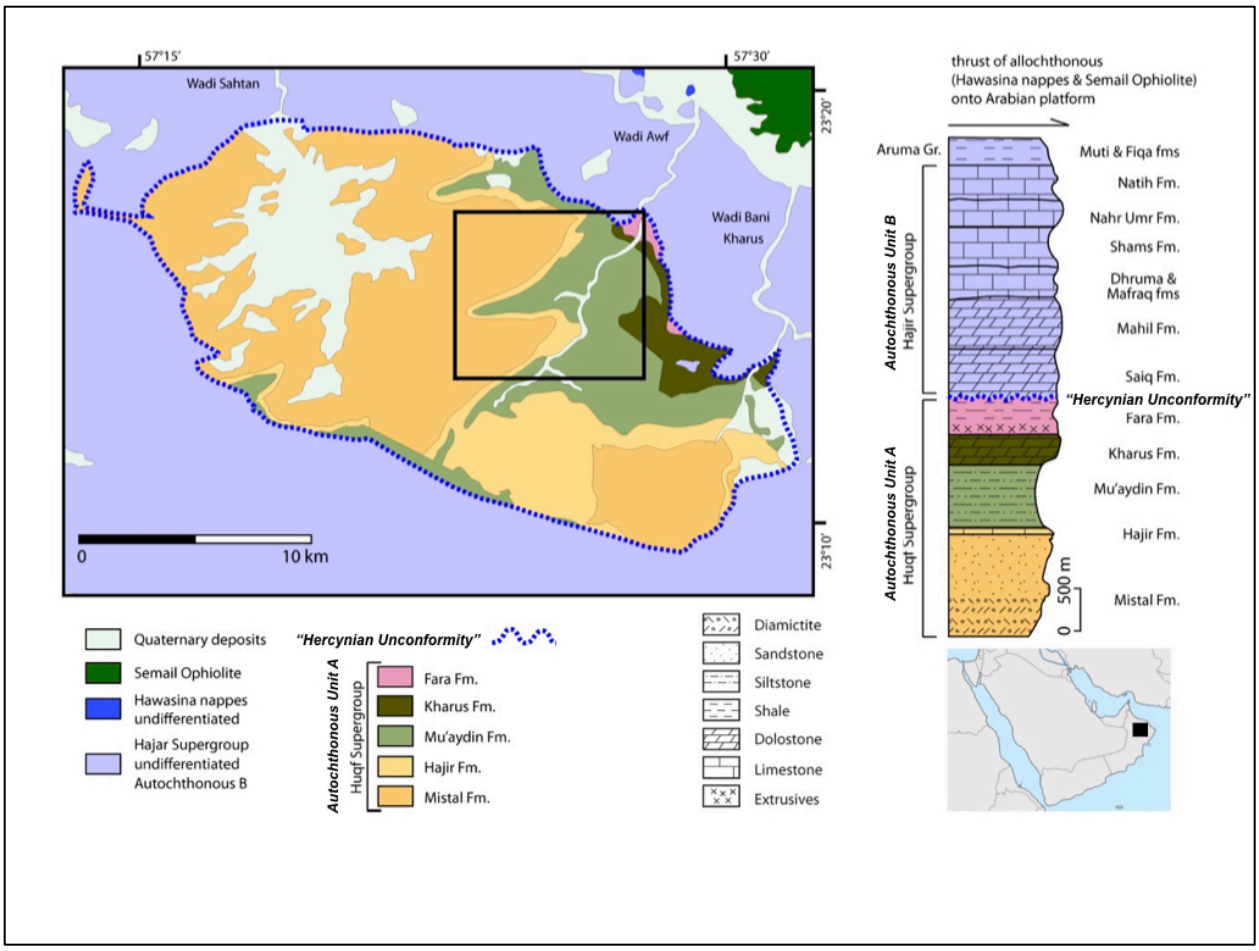

Fig. 2. Geological map and stratigraphic column of the study area (black rectangle), modified after Beurrier et al. (1986) and Béchennec et al. (1993). On the bottom right the location of the study area is shown in the context of the Arabian Peninsula.

The Oman Mountains at the northeastern margin of the Arabian Plate show an extraordinary geological record revealing several deformation events since the Proterozoic (e.g., Glennie et al., 1974). The Angudan event represents such an early (early Cambrian) deformation interval, during which a ~NW-SE-directed compressional event (in present coordinates; Droste, 2014) affected northern Oman, related to the collision between East and West Gondwana (~540-520Ma; Loosveld et al., 1996; Al-Husseini, 2000; Immerz et al., 2000; Koopman et al., 2007; Forbes et al., 2010; Al-Kindy and Richard, 2014; Droste, 2014 his Fig. 6a).

The Angudan event was caused by transpression during later stages of the Malagasy (East African) Orogeny which lasted from 550 to 510Ma (Immerz et al., 2000; Koopman et al., 2007; Droste, 2014 his Fig. 6a) and it has been correlated with a major tectonic belt along the western margin of the South Oman Salt Basin ("Western Deformation Front"; Loosveld, 1996; Bowring et al., 2007).

According to Al-Husseini (2014), the age for the Angudan event or Unconformity is 525 ±5Ma, and may correlate with the “Lower Cambrian Peneplain” (also “Afro-Arabian

142 Peneplain") which has been documented across the Middle East and North Africa (e.g., Stern et
143 al., 2006; Miller et al., 2008, respectively).
144 Crystallization ages of chlorite of 329 ±11 and 321 ±10Ma from the Neoproterozoic
145 Mu'aydin Formation of the Jabal Akhdar area (Beurrier et al., 1986) coincide with the Late
146 Paleozoic Hercynian Orogeny centered in Europe. In addition, WSW/ENE to SSW/NNE-oriented
147 folds within Neoproterozoic rocks of the Jabal Akhdar area predate Late Cretaceous obduction
148 (Mann and Hanna, 1990), which ensued sub-parallel to this fold orientation. To this date, these
149 folds are the only pre-Permian folds that have been identified in the Jabal Akhdar area. The
150 Autochthonous units A and B are separated by an angular unconformity (the "Hercynian
151 Unconformity"; Fig. 2). The Autochthonous Unit B is derived from the Permo-Mesozoic Arabian
152 shelf sedimentary rocks. Combined consideration of the unconformity, crystallization ages and
153 the WSW/ENE to SSW/NNE-oriented folds led to interpretations of these phenomena as an
154 expression of the "Hercynian Orogeny" (e.g., Beurrier et al., 1986), related to the collision
155 between Gondwana and Laurasia. According to Konert et al. (2001), the "Hercynian Orogeny"
156 affected the Arabian Plate from the Late Devonian to the Early Carboniferous, causing
157 exhumation of several kilometers of sedimentary rocks. Arch formation on the Arabian Peninsula
158 has also been attributed to "Hercynian deformation" (e.g., Faqira et al., 2009; Steward, 2016) as
159 well as block faulting (Beurrier et al., 1986; Rabu et al., 1986).
160 On the other hand, the "Hercynian interpretation" can be questioned because of the
161 significant Late Paleozoic distance between the Arabian Plate and the Gondwana-Laurasia
162 collision zone (e.g., Guiraud et al., 2005; Ruban et al., 2007). The unconformity between pre-
163 Permian rocks and Permian carbonates, as well as the stratigraphic gap mentioned above, could
164 alternatively have been caused by updoming associated with Cimmeria's breakoff from
165 Gondwana (Ruban et al., 2007). Moreover, the "Hercynian event" has recently been interpreted
166 to be mainly a thermal one (Abbo et al., 2018). The absence of an "Hercynian deformation"
167 mechanism leaves the WSW/ENE to SSW/NNE-oriented folds in the Neoproterozoic rocks,
168 alongside the published chlorite ages, unexplained. Folding would rather have to be attributed
169 to a compressional or transpressional episode predating such an "Hercynian event". Another
170 aspect leading to potentially ambiguous interpretations is the ~NE-SW orientation of structures
171 deemed "Hercynian", similarly to the trend of the Angudan Orogeny, according to present
172 cardinal directions (e.g., Droste 2014).
173 Northern Oman was affected by Pangea rifting during the Permian (e.g., Glennie et al.,
174 1974; Chauvet et al., 2009 and references therein), which, together with the "Hercynian event"
175 and/or the breakoff of Cimmeria from Gondwana resulted in the Permian Unconformity. This led
176 to the breakoff of Cimmeria from Gondwana.
177 The Permo-Mesozoic passive margin stage of the Arabian Platform was followed by the
178 Late Cretaceous Semail Ophiolite obduction. Deep marine Neo-Tethyan ocean sediments
179 (Hawasina Unit) were thrusted along with the ophiolite from the NE to the SW onto the
180 autochthonous Arabian Platform (e.g., Glennie et al., 1973, 1974; Searle and Malpas, 1980;
181 Lippard et al., 1986; Searle and Cox, 1991; Hacker et al., 1996; Goffé et al., 1998, Glennie, 2005).
182 This last is represented mainly by Permo-Mesozoic carbonates of ~3km thickness (Béchennec et
183 al., 1992; Autochthonous Unit B; Fig. 2), accumulated on the Tethyan shelf of Arabia's passive
184 margin prior to the Late Cretaceous obduction of the Tethys-derived oceanic crust and mantle of
185 the Semail Ophiolite.

Obduction was followed by extension (e.g., Mann et al., 1990; Fournier et al., 2006; Searle, 2007; Mattern and Scharf, 2018; Grobe et al., 2018, 2019) as indicated by extensional faults, which displaced the ophiolite (Mann et al., 1990; Searle, 2007). It is worth mentioning that both SHD and JAD display large-scale listric normal faults bounding their flanks (Searle, 2007). Normal faulting was likely active during the latest stage of Late Cretaceous compressional deformation associated with the ophiolite emplacement, and could have also accommodated some amount of mid-Cenozoic uplift of SHD and JAD (Searle, 2007).

The final doming of the JAD occurred from Eocene to Miocene (Hansman et al., 2017, 2018; Grobe et al., 2018, 2019). This process was accompanied by extensional shearing at the northern and eastern margin of the dome (Mattern and Scharf, 2018; Scharf et al., 2019), and tilting of the Arabian rocks along a WNW-ENE trending rotation axis at the northern and southern margin of the dome by ~30° and ~20°, respectively (compare Beurrier et al., 1986; Rabu et al., 1986).

3. Field survey and results

We divided our field area into six sectors/areas for easier comparison and geometrical reconstruction of the regional folds (Fig. 3). Our work was supported by interpretation of remote sensing data of satellite imagery at different scales available from free access databases.

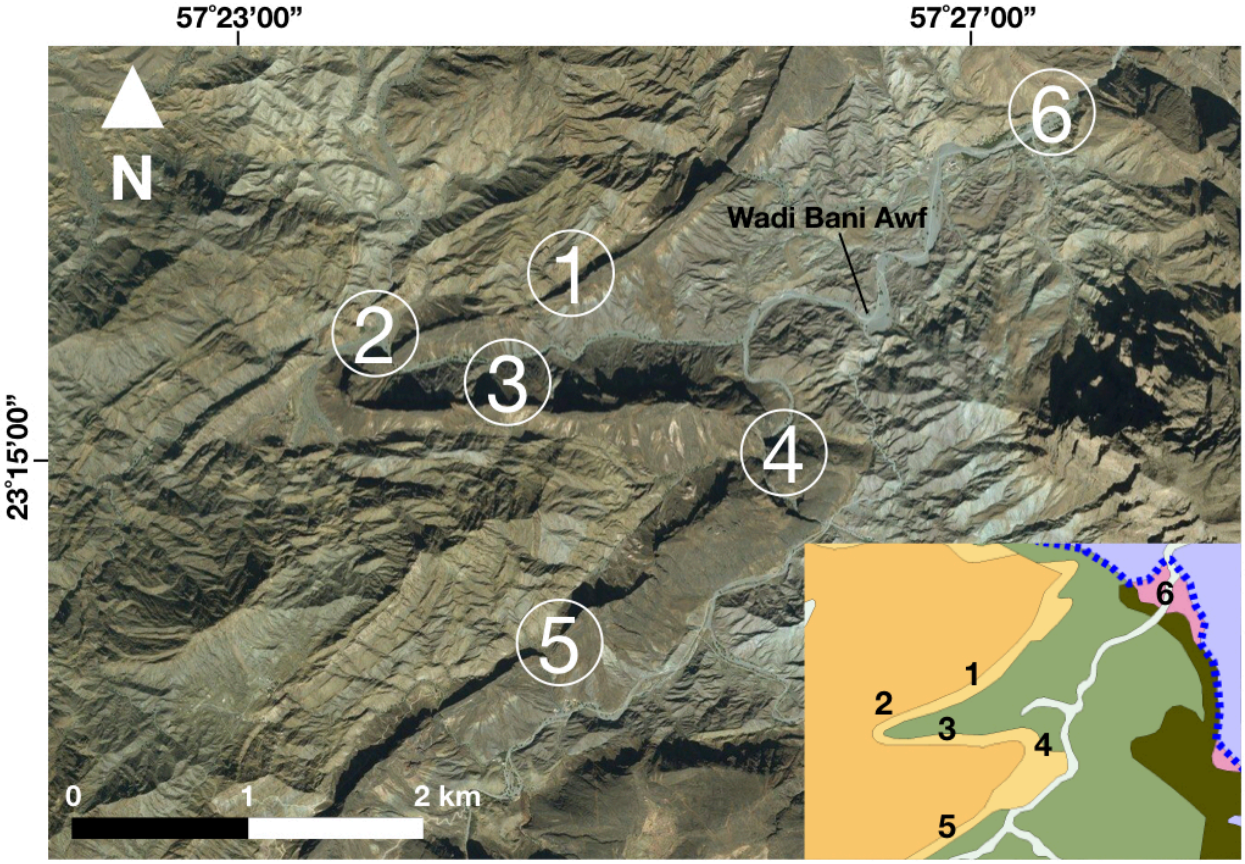

Fig. 3. Satellite imagery (Image © 2019 CNES/Airbus) of the study area with the locations of the six sectors for the structural analysis (see Fig. 2 for localization). Inlet at the lower right corresponds to the geological map of Figure 2 with respective sectors.

Sectors 1 and 5 follow a regional fold visible by satellite imagery (Fig. 3). The entire Hajir Formation has been unambiguously affected as well as the contacts with the underlying Mistal Formation and the overlying Mu'aydin Formation. These sectors follow the Hajir Formation, previously considered to be folded by “Hercynian deformation” at a regional scale (section 2; Beurrier et al., 1986). Sector 6 is located within the Fara Formation, whose lower and upper parts yield ages of 547.23 ±0.28Ma and 542.54 ±0.45Ma, respectively (Bowring et al., 2007). Thus, the very top of this formation may be of an early Cambrian in age (541Ma or younger).

3.1. Sector 1

The Hajir Formation contains numerous apparent cylindrical folds with an amplitude of a few to several meters. From the geometrical point of view we relate these folds to the first event/interval of deformation ("F1"). These ductile folds are tight (within limestone) as shown by thinned limbs and thickened hinges (Fig. 4). The F1 fold axial planes gently dip mainly towards NW and, thus, have a general vergence to the SE. The sub-horizontal fold axes trend consistently parallel to the Hajir/Mu'yadin contact (NW/SE-ward, parallel to the northern limb of the “Hercynian syncline”; S2; Fig. 5). The bedding plane within the Muaydin Formation is steeply dipping towards SE.

Two sets of cleavage occur within the silty Mu'aydin Formation. The first generally dips towards NW with a low dip angle (between 5˚ to 20˚; hereafter "S1"). The second set steeply dips (~85˚) NW-wards (hereafter "S2"). Cleavages of the second set cut those of the first. Thus, we consider the cleavage with a lower dip angle as having formed during the "D1" event, while the steeply dipping cleavage represents the "D2" event.

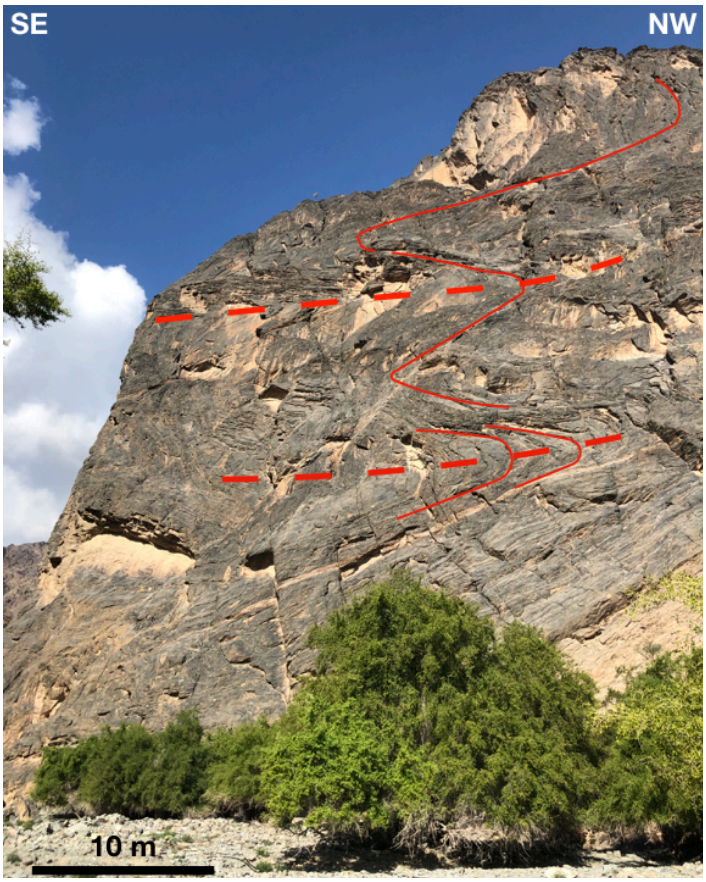

Fig. 4. Photograph of F1 folds in Hajir Formation in sector 1. Red dashed lines represent the fold axial planes of metric F1 folds, displaying a general vergence towards SE.

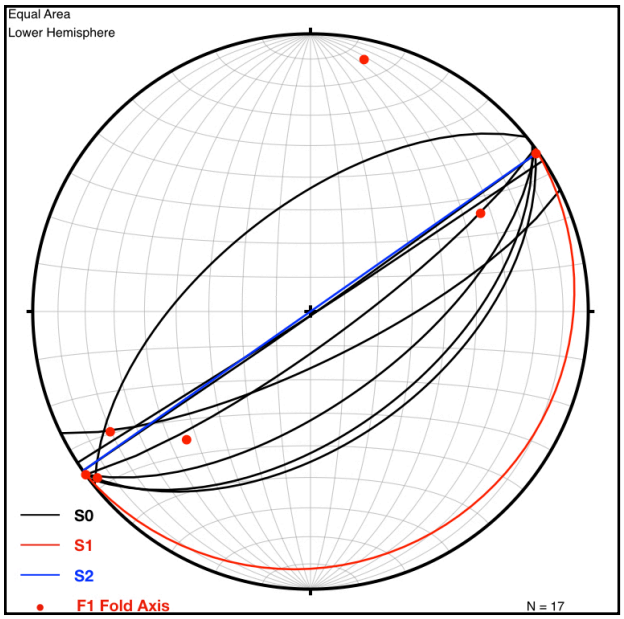

Fig. 5. Fold analysis of sector 1. S1 is the low-angle system of cleavage displaced by the sub-vertical cleavage S2.

3.2. Sector 2

Located within the hinge zone of a tight regional F2 syncline (Fig. 3), this sector is characterized by apparent cylindrical NE/SW-trending, decametric to metric F1 folds with a general vergence towards the SE. These structures are visible at the northern limb of the syncline, similarly to sector 1 folds. Sub-horizontal fold axes trend parallel to the northern limb of F2 syncline, as documented in sector 1, and therefore these F1 folds formed during the D1 event. At the southern limb of the large F2 syncline, the F1 folds are E/W-ward oriented with vergence towards the NNE (Fig. 6). In the hinge zone of a large F2 syncline (Fig. 3), the orientation of the F1 fold axes is NNW-SSE with a general vergence of the fold axial planes towards the E or ENE. Considering the systematic change of orientations of the F1 folds, it becomes reasonable to assume that the F1 folds are folded by the F2 syncline. Such syncline depicts a sub-vertical axial plane with a strike of 070° and a similarly-trending fold axis plunging 30°. The principal stress analysis of F2 data shows an almost horizontal main stress direction with a trend of N135°.

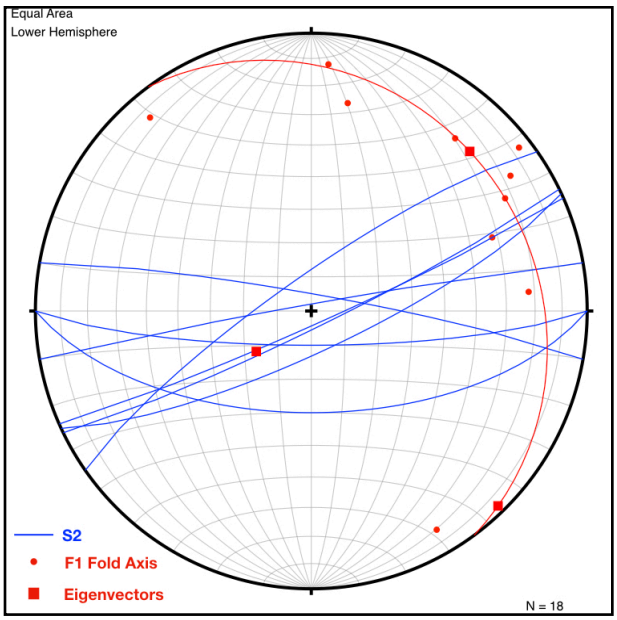

Fig. 6. Stereographic projection of F1 fold axes and D2 axial plain cleavage (S2) from sector 2. The projection depicts the change of orientation of F1 fold axes by the D2 event alongside the axial plane S2 cleavage. Eigenvectors for the main stress directions: σ1 Trend = 045.0 Plunge = 19.9; σ2 Trend = 136.0 Plunge = 2.8; σ3 Trend = 233.8 Plunge = 69.9. Best fit plane for F1 fold axis plots (red great circle) Strike = 323.8, Dip = 20.1.

3.3. Sector 3

This sector is characterized by sub-horizontal ~WNW/ESE-trending apparent cylindrical F1 folds with a general vergence towards the NNE. These folds are characterized by shallow to gently southward-dipping axial planes. The F1 folds are overturned, as seen at the contact between the older Hajir and younger Mu'aydin Formations (Fig. 7).

Fig. 7. Overturned contact between the older Hajir and younger Mu'aydin Formations in sector 3. The photograph depicts an overturned limb of an anticline with a vergence towards the NNE. Note person for scale inside the red circle.

Sector 3 is located at the southern limb of the regional F2 syncline or northern limb of the regional F2 anticline (Fig. 3). Along this limb, the vergence of the F1 folds is opposite to that of sector 1, at the northern limb of the large F2 syncline. In sector 3 and within the Mu'yadin Formation, the sub-vertical D2 cleavage is strongly developed. This cleavage strikes sub-parallelly to the F2 fold axial plane (i.e., ENE-WSW) and cuts the shallow to gently SW-ward dipping D1 cleavage. Geometrical relationship point towards D2 as the fold axial plane cleavage of F2 (Fig. 8). The principal stress analysis of this data reveals an almost horizontal main component with a trend of N175°.

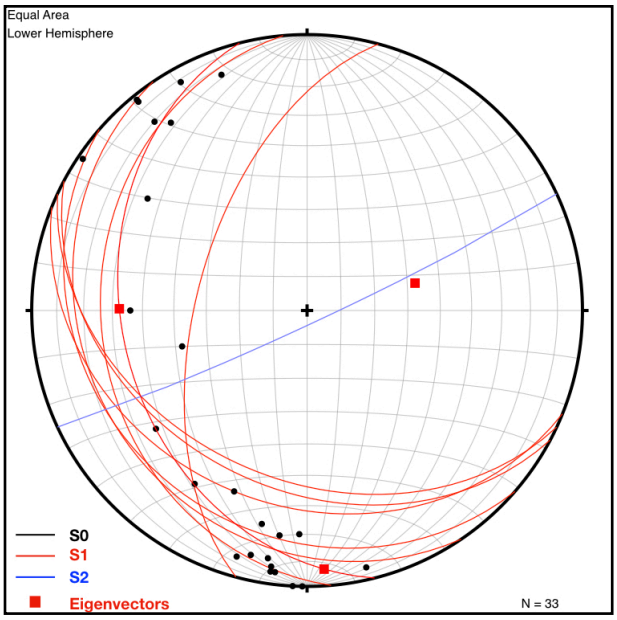

Fig. 8. Stereographic projection of foliations associated to D2 event with a fold axis trending N70 and plunging toward SE, measured in Sector 3. The D2 axial plane cleavage strikes sub-vertically towards the NE. Eigenvectors for the main stress directions: σ1 Trend = 176.2 Plunge = 6.8, σ2: Trend = 270.5 Plunge = 32.3, σ3: Trend = 075.8 Plunge = 56.8. Best fit plane for S0, strike = 165.8, Dip = 33.2.

3.4 Sector 4

F1 folds with an amplitude of ~50m are characteristic for this sector in the hinge of the D2 anticline (Fig. 3). The S1 cleavage consists of a low-dip angle and a general dip direction towards the WSW with an ENE vergence (Fig. 9).

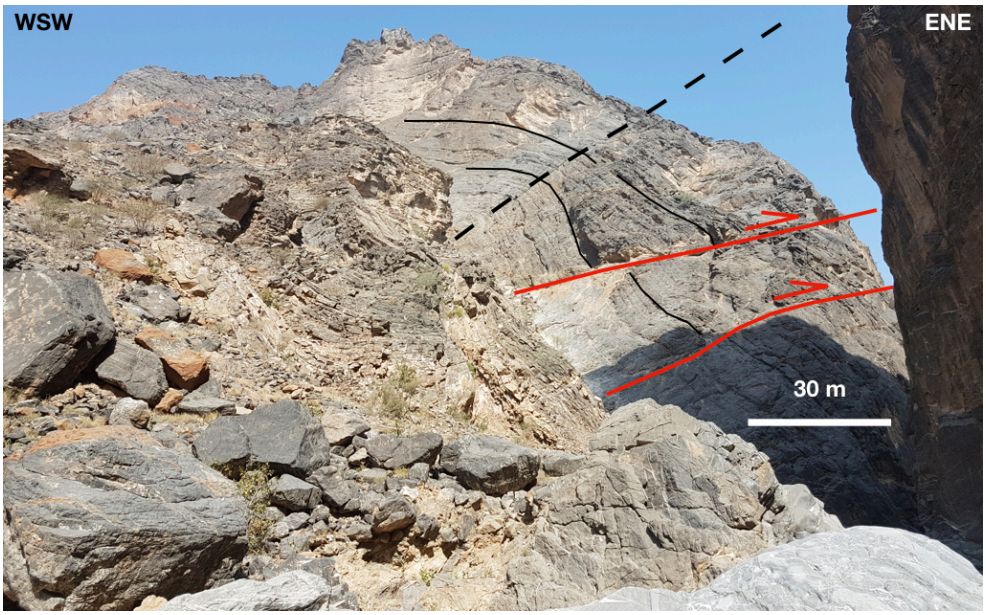

Fig. 9. Photograph of the Hajir Formation in sector 4. F1 vergence is towards ENE; F1 sub-horizontal fold axes plunge towards WNW (around N340˚) and F1 fold axial planes (red dashed line) dip 45˚ or less to WSW. Two thrusts with orientation 220/30 (dip direction/dip angle) and direction of transportation towards the NE (D1 event) are visible.

The F1 fold axes are sub-horizontal with a N-S trend. At the northern and southern limbs of the F2 anticline, the F1 fold axes are ~E-W and ~NE-SW trending, respectively (Fig. 7). Furthermore, the steeply dipping, ENE/WSW-striking F2 fold axial plane cleavage is well developed (Fig. 11).

F1 folds are associated with D1 WSW-ward dipping thrusts (Fig. 10) whose planes are localized within ≤50cm thick carbonate shear zones of the Hajir Formation (Fig. 10a, b). In spite of being formed under ductile conditions, these planes received a brittle overprint linked to an extensional event with a direction of transport to the SW.

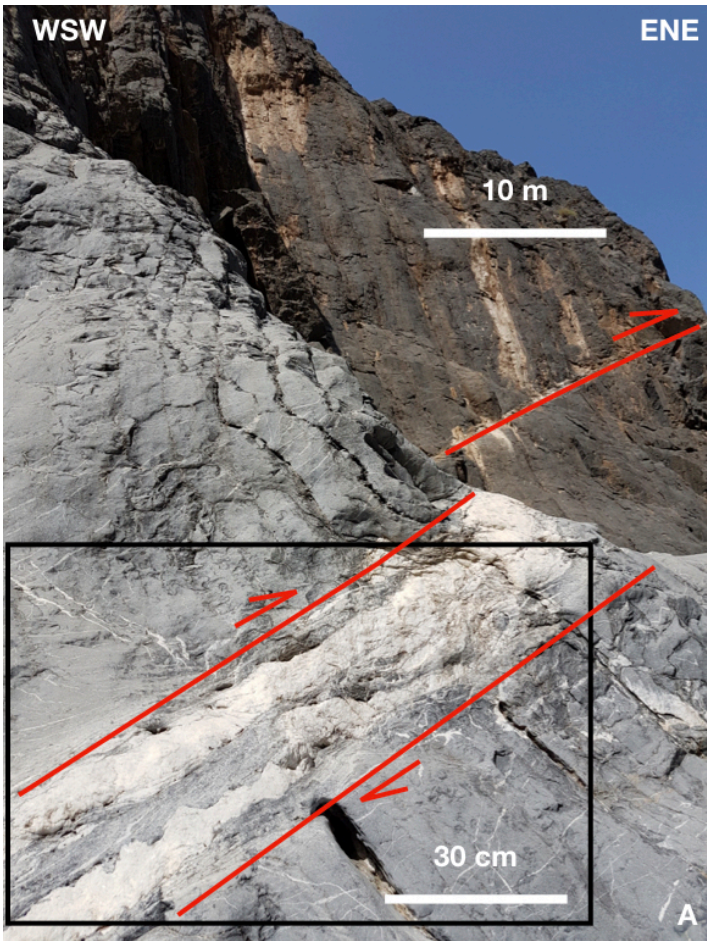

Fig. 10. Landscape view of the ENE-verging thrust with a close-up of the shear zone. The thrust has an orientation of 220/40 (dip direction/dip angle) and a transport direction toward NE (D1).

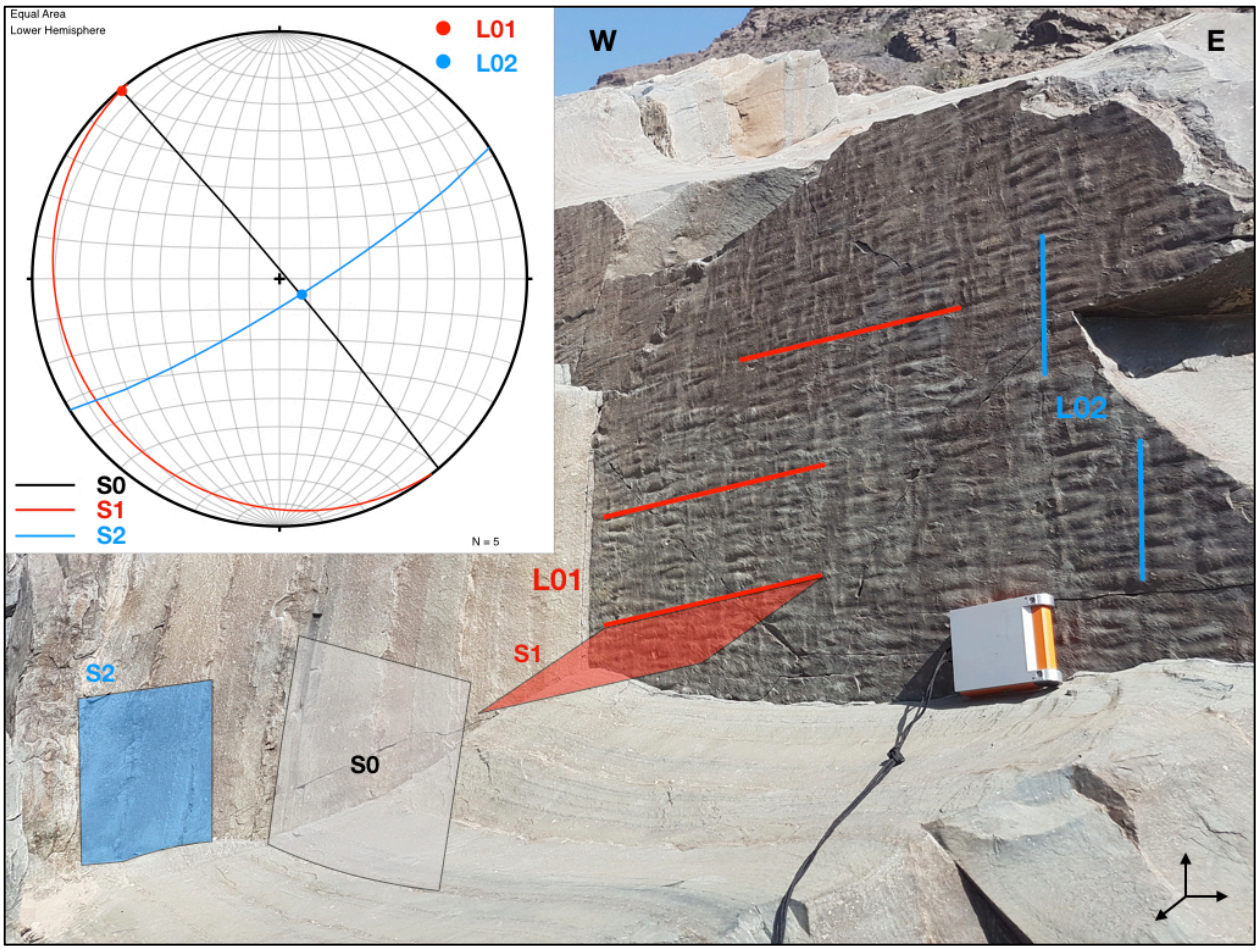

Fig. 11. Sector 4, outcrop with an unambiguous relationship of S0 (sub-vertical dip with strike N315°), S1 with a low angle dip direction toward SW and a sub-vertical S2, with a strike of N45. L01 - intersection lineation between S0 and S1; L02 - intersection lineation between S0 and S2.

3.5. Sector 5

This sector is characterized by an F1 fold with ~100m of amplitude and an axial plane dipping ~45˚ to the NW (Fig. 12). Thus, the F2 vergence is towards the SE. The F2 limb is overturned and bordered by a NW-dipping reverse fault, striking N45°, whose assignment to D1 or D2 is uncertain because of its subparallel orientation with respect to the F1 fold axial planes. The hanging wall consists of the older Mistal Formation while the footwall consists of the younger Hajir Formation.

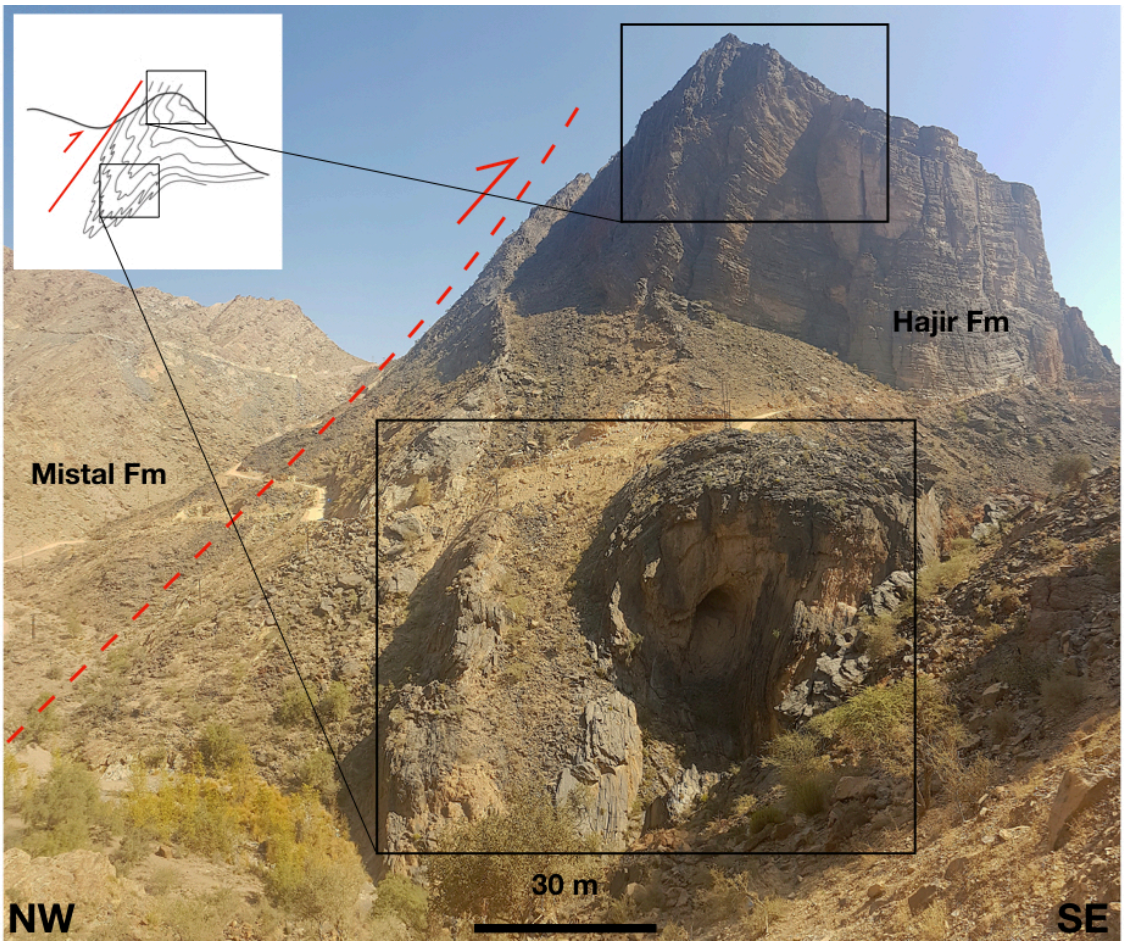

Fig. 12. Sector 5, NW dipping reverse fault marks the contact between the overturned Mistal Formation in its hanging wall and the intensely folded Hajir Formation in its footwall.

3.6. Sector 6

This sector lies within Kharus and Fara formations, which include the youngest lithologies of the Autochthonous Unit A (Fig. 2). Sector 6 is characterized by two systems of cleavages, comparable with those of sectors 1 to 5. The tight folds (F1) are apparently cylindrical and have an amplitude of a few meters. The F1 fold axial planes dip shallow to moderately towards the NW in the southern part of the outcrops, and towards SE close to the Permian Unconformity in the north (Fig. 13). The F1 folds are refolded by an open F2 syncline with an amplitude of some hundred meters (Fig. 13). The axial plane of the F2 fold is 160/85 (dip direction/dip angle; Fig. 13).

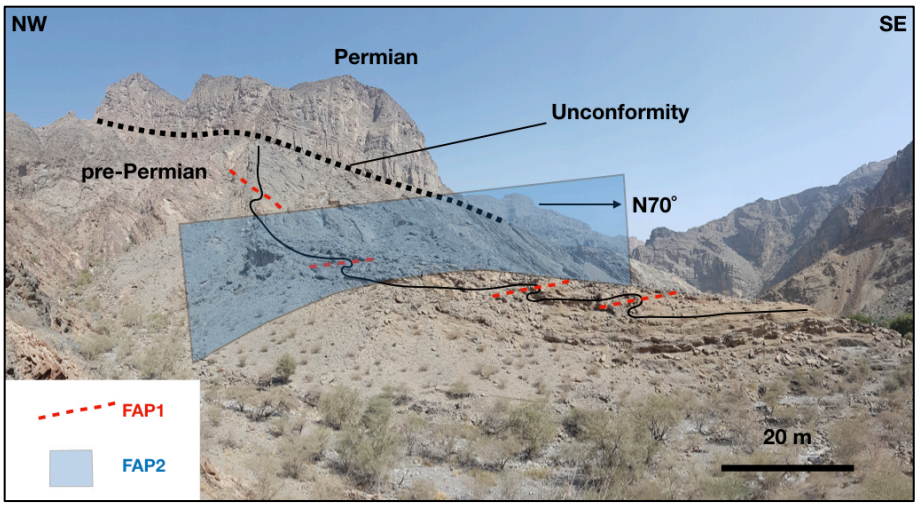

Fig. 13. In Sector 6, beneath the Permian Unconformity, the rocks of the Kharus and Fara formations are affected by F1 metric folds with axial planes that change in orientation. In the northwestern sector, they are dipping to the SE, in the southeastern sector to the NW. The F1 folds are refolded by an open F2 syncline with an axial plane steeply dipping towards the SE displaying a strike N70˚.

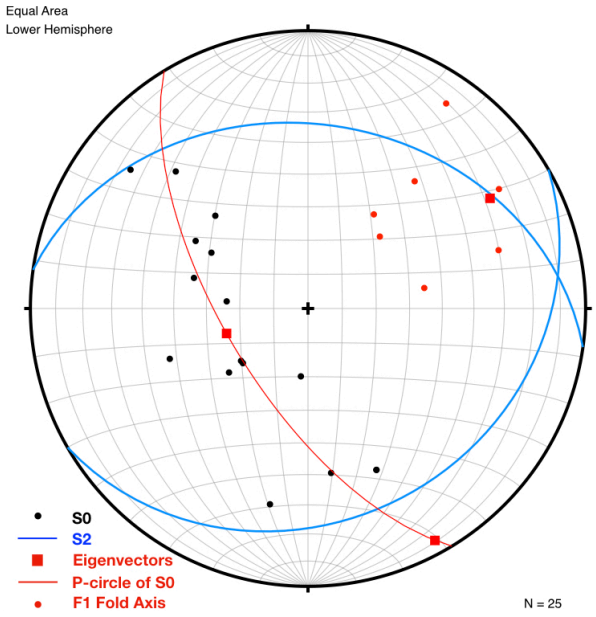

Fig. 14. Sector 6. Stereographic projection with a slight change of orientation of F1. The plot of the π -axis of the S0 poles mimics a fold axis trending to ~60˚ and plunging with 24˚. The main stress direction is sub-horizontal with a trend of 150˚. Eigenvectors for the main stress directions: σ1 Trend = 253.0 Plunge = 65.0, σ2 Trend = 151.3 Plunge = 5.4, σ3: Trend = 058.8 Plunge = 24.4. Best fit plane: Strike = 148.8, Dip = 65.6.

4. Discussion

Two different sets of folds have been identified within the western part of the Jabal Akhdar Dome (F1 and F2). These folds are schematically depicted in Figure 15, showing the F1

and F2 fold axes together with the corresponding axial planes, while Figure 16 models the two-fold sets in a steric diagram.

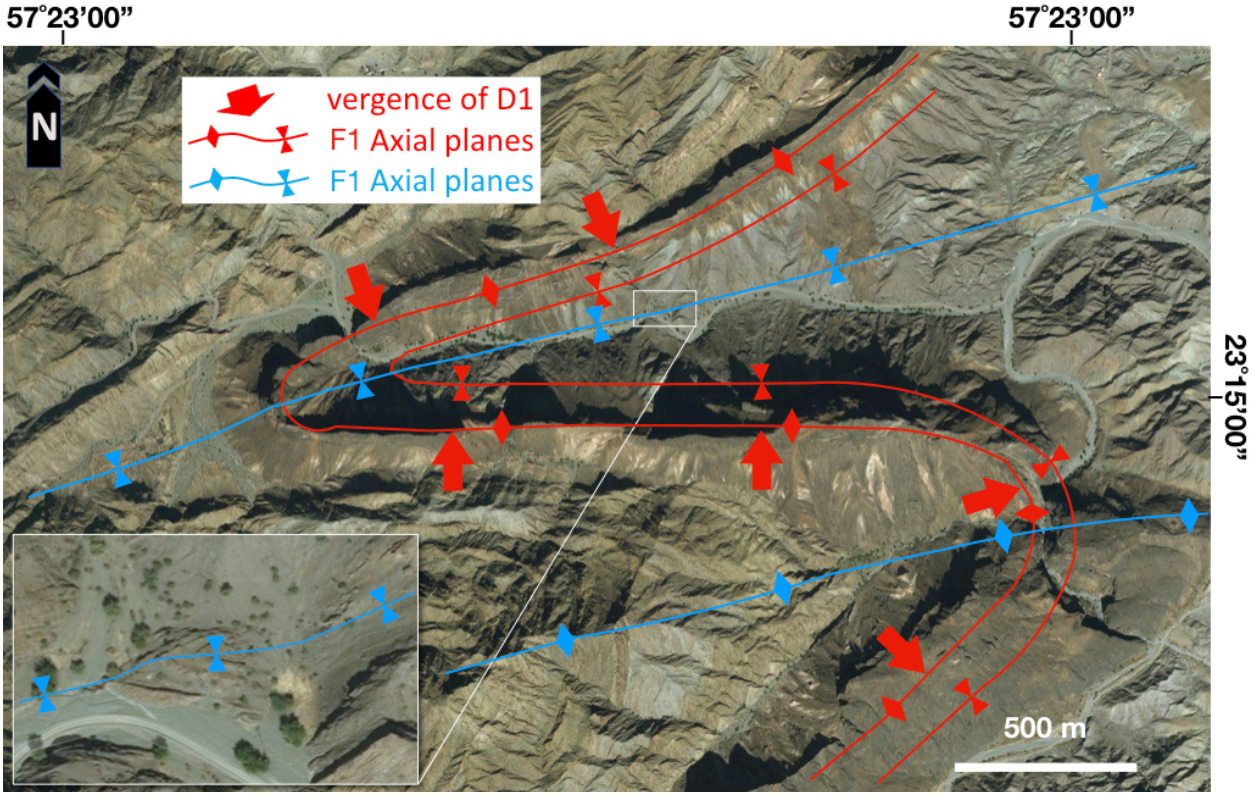

Fig. 15. Satellite imagery of the study area (Image © 2019 CNES/Airbus) focused between sectors 1 to 4. The D1 axial planes are folded by the D2 event, and the vergence of the F1 folds changes along the limbs of the F2. The small rectangle in the lower left depicts the hinge zone of the F2 with the track of the corresponding axial plane. The long side of the rectangle is equivalent to ~100m.

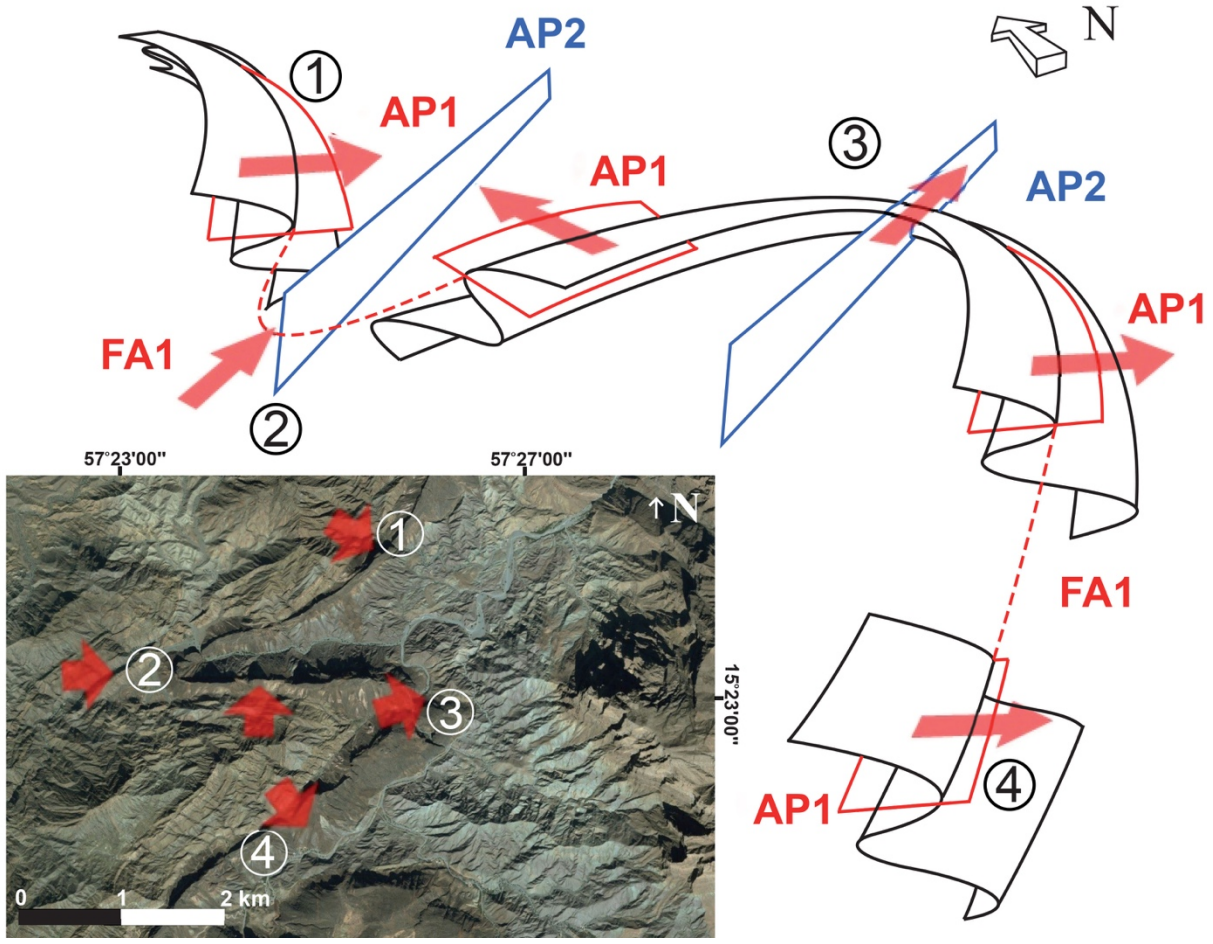

Fig. 16. Schematic depiction of the two-fold sets in the western Jabal Akhdar Dome. Numbers in the satellite image inset correlate to the numbers in the schematic sketch. FA = fold axis; AP = fold axial plane. Gentle dipping AP1 is folded by a sub-vertical AP2. Red arrows indicate direction of F1 vergence.

4.1 F1 folds

The cylindrical F1 folds are tight with an amplitude of several meters to tens of meters. The F1 folds are best visible in the limestone of the Hajir Formation. The F1 fold axes are sub-horizontally plunging and the axial planes are shallow to gently dipping. At sector 4, F1 hinges are truncated by ductile shear zones and thrusts. The mutual geometrical relation between the two events indicates that sigma 1 during F1 formation was ~NE/SW-directed, while the fold vergence is towards the NE. Some F1 folds show thickened hinges and thinned limbs, pointing towards ductile conditions prevailing during folding, with temperatures exceeding 150-250°C within limestone (compare with Kennedy and White, 2001).

We suggest that the D1 event was part of a fold-and-thrust belt considering the shallow-dipping F1 fold axial planes, the D1 thrusts, the consistent D1 vergence towards the NE, and the intense ductile deformation of the Hajir Formation limestone. Assuming a normal crustal geothermal gradient of 30°C/km, such ductile D1 deformation occurred at ~10km depth. F1 structures were exhumed and the thrust might have been reactivated as brittle extensional

faults. The direction of transport during extension was ~SW and the temperature was cooler than 150-250°C (compare Kennedy and White, 2001).

4.2 F2 folds

Since the large-scale F2 folds have been already described in previous studies (e.g., Beurrier et al., 1986; Mann and Hanna, 1990), we wish to point out their differences with respect to F1, while stressing the main F2 characteristics. The F2 folds have a much larger amplitude than F1 (F1: few meters to tens of meters; F2: few kilometers), their axial planes are sub-vertically oriented and strike ~ENE-WSW (with local minor changes), therefore indicating a sub-horizontal ~NNW-SSE-oriented sigma 1. The F2 fold axes plunge ~55-60° to ENE, but however, the rocks in our study area have been rotated ~30° along a WNW/ENE-trending rotation axis during Cenozoic D3 doming (see Fig. 17 and section 2). Thus, a back-rotation of F2 axes would indicate an original plunge of 25-30° (Fig. 16). F1 and F2 folds formed during highly oblique variants of sigma 1 (sigma 1 for F1: ~NE-SW; sigma 1 for F2: ~NW-SE). Ductile conditions during F2 activity were probably of the same order of magnitude as for the F1 folds, taking into account the style of F2 folds within limestone. The absolute age of the F2 folds is unknown, however, their orientation is parallel to the Angudan Orogen (Fig. 18). In any case, The F2 folds are younger than F1 and older than the Permian Unconformity (see above). Hence, we rule out the occurrence of an "Hercynian" folding event associated to F2, due to the significant distance between the eastern Arabian Plate and the collision zone during the Late Paleozoic (see section 2), even though the "Hercynian" and Angudan directions of convergence were sub-parallel. Moreover, map analyses reveal that the Cambro-Ordovician Amdeh Formation of the Saih Hatat Dome lack NE/SW-directed folds (Villey et al., 1986; Béchennec et al., 1992), suggesting that folds of this trend predate deposition of the Amdeh Formation and, thus, the Carboniferous "Hercynian Orogeny".

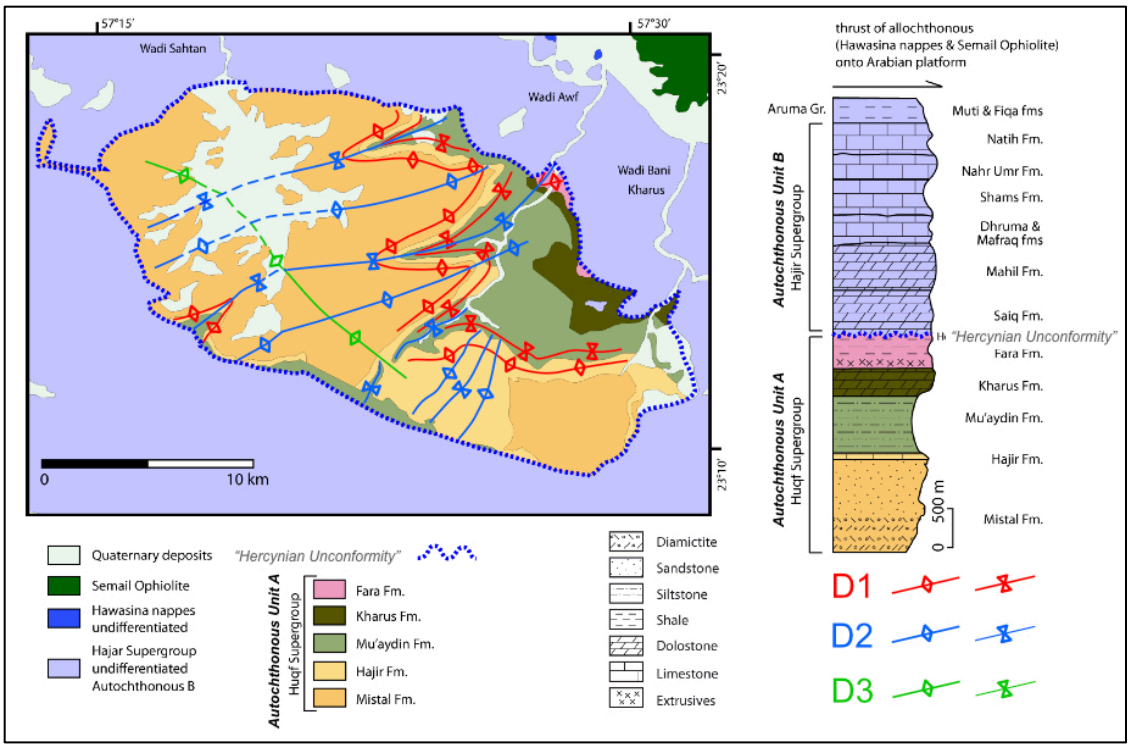

Fig. 17. Schematic structural map of the study area modified after Beurrier et al. (1986) and Béchennec et al. (1993).

4.3. Regional and temporal implications

We suggest that the D1 event is a result of the convergence between a microcontinent ("NW Iran" or "Iran"?) with Arabia (see Jacobs et al., 2008, their Fig. 1a; Hu et al., 2017, their Fig. 11a), or related to the consumption of Proto-Tethys oceanic lithosphere beneath those microcontinents and Arabia (see Jacobs et al., 2008, their Fig. 1a; Hu et al., 2017, their Fig. 11a). Regardless of the process, the direction of convergence for both scenarios was NE-SW (in present coordinates; e.g., Jacobs et al., 2008) which resulted in the formation of the NW/SE-oriented F1 folds (Fig. 18). The age of the compressional event is not specified, but, nevertheless, the Proto-Tethyan subduction age is in the range of 557-516Ma (Hu et al., 2017, their Fig. 11a).
The deposition of Fara Formation lasted until ~542Ma (Bowring et al., 2007) and the Angudan event has an age of 525 ±5Ma (Al-Husseini, 2014). This major deformation occurrence is evidenced by NW-SE contraction (Droste, 2014) to which we assign the D2 event. Therefore, the NE/SW-directed event (D1) firstly affected the Arabian Plate at some time between ~542Ma and 525 ±5Ma (Fig. 18).

Occurrences of calc-alkaline magmatism and the associated continental arc setting at the Ediacaran-Cambrian transition (~572 to 528Ma) have been reported for neighboring Iranian Terranes (e.g., Rosetti et al., 2015; Moghadam et al., 2017 and references therein). This tectonic environment is contextual with the Cadomian Orogeny (e.g., Rosetti et al., 2015).

We relate the D1 NE/SW-directed compressional event, forming the NW/SE-oriented F1 folds which affected northeastern Oman between ~542 and 525 ±5Ma to the Cadomian

Orogeny. Consequently, the shallow dip and the NW-directed vergence of F1 fold axial planes were acquired in the course of a fold-and-thrust-belt deformation during the Cadomian Orogeny.

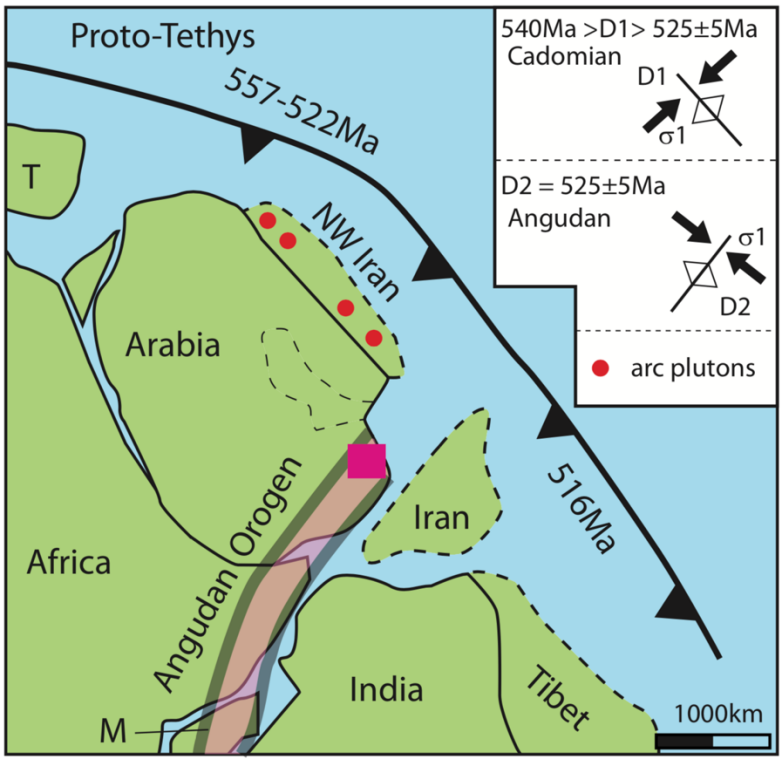

Fig.18. Geological setting of Greater Arabia at the Precambrian/Cambrian boundary modified after Jacobs et al. (2008) and Hu et al. (2017). M – Madagascar; T – Turkey. Ages of the Andean-type subduction zone of the Proto-Tethys Ocean beneath Gondwana are from Hu et al. (2017). This subduction zone is part of the Cadomian Orogeny (e.g., Rossetti et al., 2015). The red semi-transparent stripe marks the Angudan Orogen (after Droste, 2014). Red rectangle indicates the study area. Note that several authors indicate microcontinents with different positions between Arabia and the subduction zone under different designations. For instance, “Iran” of Jacobs et al. (2008) is "Afghan Block" in Droste (2014), and "Afghan-NW Pakistan" in Hu et al. (2017). Arc plutons simplified after Moghadam et al. (2016). Inset summarizes the timing and kinematics of the Cadomian and Angudan events in our study area. The Cadomian event postdates the deposition of Fara Formation and is associated with the closure of the Proto-Tethys Ocean or accretion of a microcontinent. The Angudan event is associated with East and West Gondwana joining to form the main part of Gondwana.

The style of D2 deformation within the Neoproterozoic/Early Cambrian formations differs between the western and eastern part of the Jabal Akhdar Dome. In the western part of the Jabal Akhdar Dome (sectors 1-5), the F2 folds are tight and clearly visible with an amplitude of few kilometers (Fig. 17). The fold axes trend ENE-WSW. Towards the East and Northeast (sector 6), the style of the F2 folds changes. The F2 folds are more open with an amplitude of a few hundred meters and an orientation of the fold axes of NE-SW (Fig. 17). The orientation of the F2 folds changes from WSW-ENE in the Northwest of the study area to SSW-NNE in the Southeast. We relate these changes in style and orientation to heterogenous strain caused by the northern termination of the Angudan Orogeny near our study area (Fig. 18).

5. Conclusions

This study describes for the first time two early Paleozoic fold structures within the western part of the Jabal Akhdar Dome. The earlier fold set involves amplitudes of several meters, sub-horizontal fold axes and shallow-dipping fold axial planes, formed during a NE/SW-directed compressional event. F1 folds are associated to local thrusts and shear zones within limestone, whose deformation occurred at ≥150-250°C. These folds have been correlated with an earliest Cambrian event caused by NE/SW-directed convergence of a microplate with Arabia or with a subduction zone, consuming Proto-Tethys oceanic lithosphere. The D1 structures may be part of a fold-and-thrust-belt which formed during the Cadomian event, postdating the deposition of Fara Formation (~542Ma) and predating the Angudan Orogeny (525 ±5Ma).

According to the geological map by Moghadam et al. (2016), arc plutons related to the Cadomian/Peri-Gondwanan subduction zone occur in southwestern Iran, and our study area should accordingly be situated on the upper plate (Fig. 18). Considering that this arc paralleled the subduction zone along the active margin, the distance between this arc and the study area amounts to ~500km, disregarding later shortening of the Zagros Mountains. Thus, our study area very likely represents a retroarc fold-and-thrust belt. This idea is also supported by the sedimentary lithologies belonging to Neoproterozoic formations at the studied area (Fig. 2), as well as by Fara Formation volcanic sequences broadly consistent with subduction-related melting of the crust in a retroarc setting (Grotzinger et al., 2002). From the study area to the Northeast, one can expect the presence of arc magmatites in the subsurface. Considering the fact that subduction had occurred between 557-516Ma (Fig. 18; Hu et al., 2017), extension at the transition between the Hajir and Mu'aydin Formations at ~600 to ~590Ma (Mattern and Scharf, 2019) predates the Cadomian subduction.

The F1 folds are deformed by large-scale (several kilometers in amplitude) F2 folds. These folds developed ~WSW/ESE-striking sub-vertical axial planes with gently plunging fold axes towards the NE. The fold axes of the F1 folds are parallel to the limbs of the F2 folds.

The F2 folds formed during the NW/SE-oriented Angudan compression. We rule out effects of the "Hercynian Orogeny" for the F2 folds because of the significant distance between our study area and the Hercynian collision zone during the Late Paleozoic. The Hercynian event in eastern Arabia was a thermal effect without significant folding. However, large-scale arch formation and block faulting may have been present during the Hercynian event.

Acknowledgment

This research did not receive any specific grant from funding agencies in the public, commercial, or not-for-profit sectors. We are indebted to Giulio Viola (University of Bologna, Italy) for fruitful discussions on the field. We thank the editor xxx as well as the reviewers xxx and xxx for their critical comments. Tectonic data were plotted with R.W. Allendinger's software (Stereonet, version 10.2.9).

References

Abbo, A., Avigad, D., Gerdes, A., 2018. The lower crust of the Northern Arabian Shield (N Israel): Neoproterozoic sediment subduction and syn-Variscan thermal imprint from U-Pb-Hf in zircons from granulite xenoliths. EGU 2018-4596, vol. 20, Vienna.

Al-Husseini, M.I., 2000. Origin of the Arabian Plate Structures: Amar Collision and Najd Rift. GeoArabia 5, 527-542.

Al-Husseini, M.I., 2014. Ediacaran-Cambrian Middle East geologic time scale 2014, proposed correlation of Oman's Abu Mahara Supergroup and Saudi Arabia's Jibalah Group. GeoArabia 19, 107-132.

Al-Kindy, M.H., Richard, P.D., 2014. The main structural styles of the hydrocarbon reservoirs in Oman. In: Rollinson, H.R., Searle, M.P., Abbasi. I.A., Al-Lazki, A.I. & Al-Kindy, M.H. (Eds.), Tectonic evolution of the Oman Mountains. Geological Society, London, Special Publication 392, 409-445, doi: 10.1144/SP392.20.

Allen, P.A., 2007. The Huqf Supergroup of Oman: Basin development and context for Neoproterozoic glaciation. Earth Science Reviews 84, 139-185.

Bauer, W., Callegari, I., Al Balushi, N., Al Busaidi, G., Al Barumi, M., Al Shoukri, Y., 2018. Tectonic observations in the northern Saih Hatat, Sultanate of Oman. Arabian Journal of Geosciences 11, 94.

Béchennec, F., Roger, J., Le Métour, J., Wyns, R., 1992. Geological map of Seeb, sheet NF 40-03, scale 1:250,000, with Explanatory Notes: Directorate General of Minerals, Oman Ministry of Petroleum and Minerals.

Béchennec, F., Roger, J., Le Métour, J., Wyns, R. 1993. Geological Map of Seeb, Sheet NF 40-03, 1:250,000 with Explanatory Notes, Ministry of Petroleum and Minerals, Muscat.

Beurrier, M., Béchennec, F., Rabu, D., Hutin, G., 1986. Geological map of Rustaq, sheet NF 40-03D, scale 1:100,000, with Explanatory notes: Directorate General of Minerals, Oman Ministry of Petroleum and Minerals.

Bowring, S.A., Grotzinger, J.P., Condon, D.J., Ramezani, J., Newall, M., Allen, P.A., 2007. Geochronologic constraints of the chronostratigraphic framework of the Neoproterozoic Huqf Supergroup, Sultanate of Oman. American Journal of Science 307, 1097-1145, doi: 10.2475/10.2007.01.

Brasier, M., McCarron, G., Tucker, R., Leather, J., Allen, P., Shields, G., 2000. New U-Pb zircon dates for the Neoproterozoic Ghubrah glaciation and for the top of the Huqf Supergroup, Oman. Geology 28(2), 175-178.

British Geological Survey, 2006. Geological map of the Northern Emirates, 1:250,000 scale. British Geological Survey, Keyworth.

Chauvet, F., Dumont, T., Basile, C., 2009. Structures and timing of Permian rifting in the central Oman Mountains (Saih Hatat). Tectonophysics 475, 563-574.

Droste, H., 2014. Petroleum geology of the Sultanate of Oman. In: Marlow, L., Kendall, C., Yose, L. (Eds.), Petroleum Systems of the Tethyan Region. American Association of Petroleum Geologists Memoir 106, 713-755.

Faqira, M., Rademakers, M., Afifi, A., 2009. New insights into the Hercynian Orogeny, and their implications for the Paleozoic Hydrocarbon System in the Arabian Plate. GeoArabia 14, 199-228.

559 Forbes, G.A., Jansen, H.S.M., Schreurs, J., 2010. Lexicon of Oman subsurface stratigraphy.
560 Reference guide to the stratigraphy of Oman's Hydrocarbon basins. GeoArabia, Special
561 Publication 5 by Gulf Petro Link, 1-373.
562 Fournier, M., Lepvrier, C., Razin, P., Jolivet, L., 2006. Late Cretaceous to Paleogene post-obduction
563 extension and subsequent Neogene compression in the Oman Mountains. GeoArabia 11, 17-
564 40.
565 Glennie, K. W., 2005. The Geology of the Oman Mountains: An Outline of Their Origin, 2nd ed.,
566 Scientific Press, Beaconsfield, p. 110.
567 Glennie, K.W., Boeuf, M.G.A., Hughes-Clarke, M.W., Moody-Stuart, M., Pilaar, W.F.H., Reinhardt,
568 B.M., 1973. Late Cretaceous nappes in Oman Mountains and their geological evolution.
569 American Association of Petroleum Geologists Bulletin 57, 5-27.
570 Glennie, K.W., Boeuf, M.G.A., Highes-Clarke, M.W., Moody-Stuart, M., Pilaar, W., Reinhardt,
571 B.M., 1974. Geology of the Oman Mountains. Verhandelingen van het Koninklijk Nederlands
572 Geolologisch Mijnbouwkundig Genootschap 31, 423.
573 Goffé, B., Michard, A., Kienast, J.R. LeMer, O., 1988. A case of obduction related high P, low T
574 metamorphism in upper crustal nappes, Arabian continental margin, Oman: P-T paths and
575 kinematic interpretation. Tectonophys 151, 363-386.
576 Grobe, A., Virgo, S., von Hagke, C., Urai, J.L., Littke, R., 2018. Multiphase structural evolution of a
577 continental margin during obduction orogeny: Insights from the Jebel Akhdar Dome, Oman
578 Mountains. Tectonics 37(3), 888-913, doi: 10.1002/2016TC004442.
579 Grobe, A. von Hagke, C., Littke, R., Dunkl, I., Wübbeler, F., Muchez, P., Urai, J.L., 2019. Tectono-
580 thermal evolution of Oman's Mesozoic passive continental margin under the obducting
581 Semail Ophiolite: a case study of Jebel Akhdar, Oman. Solid Earth 10, 149-175, doi:
582 10.5194/se-10-149-2019.
583 Grotzinger, J. P., Al-Siyabi, H. A., Al-Hashmi, R., and Cozzi, A., 2002, New Model for Tectonic
584 Evolution of Neoproterozoic-Cambrian Huqf Supergroup Basins, Oman: GeoArabia
585 (Manama), v. 7, p. 241.
586 Guiraud, R., Bosworth, W., Thierry, J., Delplanque, A., 2005. Phanerozoic geological evolution of
587 Northern and Central Africa: An overview. Journal of African Earth Sciences 43, 83-143, doi:
588 10.1016/j.jafrearsci.2005.07.017.
589 Kennedy, L.A., White, J.C., 2001. Low-temperature recrystallization in calcite: mechanisms and
590 consequences. Geology, 29. 1027-1030.
591 Konert, G., Afifi, A.M., Al-Hajri, S.A., Droste, H.J., 2001. Paleozoic Stratigraphy and Hydrocarbon
592 Habitat of the Arabian Plate. GeoArabia 6, 407-442.
593 Hacker, B.R., Mosenfelder, J.L., Gnos, E., 1996. Rapid emplacement of the Oman ophiolite:
594 Thermal and geochronologic constraints. Tectonics 15, 1230-1247.
595 Hansman, R.J., Ring, U., Thomson, S.N., den Brock, B., Stübner, K., 2017. Late Eocene uplift of the
596 Al Hajar Mountains, Oman, supported by stratigraphic and low-temperature
597 thermochronology. Tectonics 36(12), 3081-3109, doi: 10.1002/2017TC004672.
598 Hansman, R.J., Albert, R., Gerdes, A., Ring, U., 2018. Absolute ages of multiple generations of
599 brittle structures by U-Pb dating of calcite. Geology 46(3), 207-210, doi: 10.1130/G39822.1.
600 Hu, P., Zhai, Q., Ren, G., Wang, J., Tang, Y., 2017. Late Ordovician high-Mg adakitic andesite in the
601 western South China block: evidence of oceanic subduction. International Geology Review
602 60(9), 1140-1154, doi: 10.1080/00206814.2017.1370617.

603 Immerz, P.W., Oterdoom, H., El-Tonbary, M., 2000. The Huqf/Haima hydrocarbon system of
604 Oman and the termianl phase of the Pan-African Orogeny: Evaporite depositions in a
605 compressive setting. 4th Middle East Geosciences Conference, GEO 2000, GeoArabia,
606 Abstract 5, 113-114.
607 Jacobs, J., Bingen, B., Thomas, R.J., Bauer, W., Wingate, M.T.D., Feitio, F.. 2008. Early Palaeozoic
608 orogenic collapse and voluminous late-tectonic magmatism in Dronning Maud Land and
609 Mozambique: insights into the partially delaminated orogenic root of the East
610 African_Antarctic Orogen? In: Satish-Kumar, M., Motoyoshi, Y., Osanai, Y., Hiroi, Y. &
611 Shiraishi, K. (eds.), Geodynamic Evolution of East Antarctica: A Key to the East–West
612 Gondwana Connection. Geological Society, London, Special Publications, 308, 69–90.
613 Konert, G., Afifi, A.M., Al-Hajri, S.A., Droste, H.J., 2001. Paleozoic Stratigraphy and Hydrocarbon
614 Habitat of the Arabian Plate. GeoArabia 6(3), 407-442.
615 Koopman, A., van der Berg, M., Romine, K., Teasdale, J., 2007. Proterozoic to Cambrian plate-
616 tectonics and its control on the structural evolution of the Ara Salt-Basin in Oman. Abstract
617 AAPG European Region Conference, Athens, Greece: AAPG Search and Discovery Article
618 #90072.
619 Lippard, S.J., Shelton, A.W., Gass, I.G., 1986. The ophiolite of northern Oman. Journal of
620 Geological Society (London) Memoir. 11, 178.
621 Loosveld, R.J.H., Bell, A., Terken, J.J.M., 1996. The tectonic evolution of interior Oman. GeoArabia
622 1, 28-51.
623 Mann, A., Hanna, S.S., 1990. The tectonic evolution of pre-Permian rocks, Central and
624 Southeastern Oman Mountains. In: Robertson, A.H.F., Searle, M.P., Ries, A.C. (Eds.), The
625 Geology and Tectonics of the Oman Region. Geological Society of London, Special
626 Publication 49, 307-325.
627 Mann, A., Hanna, S.S., Nolan, S.C., 1990. The post-Campanian tectonic evolution of the Central
628 Oman Mountains: Tertiary extension of the Eastern Arabian Margin. In: Robertson, A.H.F.,
629 Searle, M.P., Ries, A.C. (Eds.), The Geology and Tectonics of the Oman Region, Geological
630 Society London Special Publication 49, 549-563.
631 Mattern, F., Pracejus, B., Al Balushi, L. 2018. Heavy mineral beach placers of the Ordovician
632 Amdeh Formation (Member 4, Wadi Qazah, Saih Hatat, eastern Oman Mountains): Where
633 is the main source area?. Journal of African Earth Sciences 147, 633-646.
634 Mattern, F., Scharf, A., 2018. Postobductional extension along and within the Frontal Range of
635 the Eastern Oman Mountains. Journal of Asian Earth Sciences 154, 369-385, doi:
636 10.1016/j.jseaes.2017.12.031.
637 Mattern, F., Scharf, A., 2019. Transition from the Hajir Formation to the Muaydain Formation: A
638 facies change coinciding with extensional, syndepositional faulting (Ediacaran, Jabal Akhdar
639 Dome, Central Oman Mountains). Journal of African Earth Sciences 152, 237-244, doi:
640 10.1016/j.jafrearsci.2019.02.016.
641 Mercolli, I., Briner, A.P., Frei, R., Schönberg, R., Nägler, T.F., Kramers, J., Peters, T., 2006.
642 Lithostratigraphy and geochronology of the Neoproterozoic crystalline basement of Salalah,
643 Dhofar, Sultanate of Oman: Precambrian Research 145, 182–206.
644 doi:10.1016/j.precamres.2005.12.002.
645 Miller, N., Johnson, P.R., Stern, R.J., 2008. Marine versus non-marine environments for the Jibalah
646 Group, NW Arabian Shield: a sedimentologic and geochemical survey and report of possible

metazoan in the Dhaiqa Formation. The Arabian Journal for Science and Engineering 33(1C), 55-77.
Miller, C.G., Heward, A;P., Mossoni, A., Sansom, I.J., 2018. Two new early balognathid conodont genera from the Ordovician of Oman and comments on the early evolution of prioniodontid conodonts. Journal of Systematic Palaeontology 16(7), 571-593, doi: 10.1080/14772019.2017.1314985.
Moghadam, H.S., Li, X.-H., Stern, R.J., Santos, J.F., Ghorbani, G., Pourmohsen, M., 2016. Age and nature of 560-520 Ma calc-alkaline granitoids of Biarjmand, northeast Iran: insights into Cadomian arc magmatism in northern Gondwana. International Geology Review 58(12), 1492-1509, doi: 10.1080/00206814.2016.1166461.
Moghadam, H.S., Li, X.-H., Santos, J.F., Stern, R.J., Griffin, W.L., Ghorbani, G., Sarebani, N., 2017. Neoproterozoic magmatic flare-up along the N. margin of Gondwana: The Taknar complex, NE Iran. Earth and Planetary Science Letters 474, 83-96, doi: 10.1016/j.epsl.2017.06.028.
Moraetis, D., Mattern, F., Scharf, A., Frijia, G., Kusky, T.M., Yuan, Y., Hussain., I.L., 2018. Neogene to Quaternary uplift history along the passive margin of the northeastern Arabian Peninsula eastern Hajar Mountains, Oman. Quaternary Research 90(2), 418-434, doi: 10.1017/qua.2018.51.
Rabu, D., Béchennec, F., Beurrier, M., Hutin, G., 1986. Geological map of Nakhl, sheet NF40-3E, scale: 1:100,000, with Explanatory Notes: Directorate General of Minerals, Oman Ministry of Petroleum and Minerals.
Rossetti, F., Nozaem, R., Lucci, F., Vignatoli, G., Gerdes, A., Nasrabadi, M., Theye, T., 2015. Tectonic setting and geochronology of the Cadomian (Ediacaran-Cambrian) magmatism in Central Iran, Kuh-e-Sarhangi region (NW Lut Block). Journal of Asian Earth Sciences 102, 24-44, doi: 10.1016/j.jseaes.2014.07.034.
Ruban, D.A., Al-Husseini, M.I., Iwasaki, Y., 2007. Review of Middle East Paleozoic Plate Tectonics. GeoArabia 12, 35-56.
Scharf, A., Mattern, F., Moraetis, D., Callegari, I., Weidle, C., 2019. The Semail Gap Fault Zone of the Oman Mountains and its postobductional evolution. EGU 2019-4026, Vienna, Austria
Searle, M., Cox, J., 1991. Tectonic setting, origin, and obduction of the Oman ophiolite. Geological Society of America Bulletin 111, 104-122.
Searle, M.P., 2007. Structural geometry, style and timing of deformation in the Hawasina Window, Al Jabal al Akhdar and Saih Hatat culminations, Oman Mountains. GeoArabia 12, 99-130.
Searle, M.P., Malpas, J., 1980. Structure and metamorphism of rocks beneath the Semail ophiolite of Oman and their significance in ophiolite obduction. Trans. R. Soc. Edinburgh 71, 247-262.
Stern, R.J., Avigad, D., Miller, N.R., Beyth, M., 2006. Evidence for the Snowball Earth hypothesis in the Arabian-Nubian Shield and the East African Orogen. Journal of African Earth Sciences 44, 1-20, doi: 10.1016/j.afrearsci.2005.10.003.
Steward, S.A., 2016. Structural geology of the Rub' Al-Khali Basin, Saudi Arabia. Tectonics 35, 2417-2438, doi: 10.1002/2016TC004212.
Torsvik, T.H., Cocks, L.R.M., 2017. Earth history and paleogeography, Cambridge University Press, 317 p.

690 Villey, M., Le Métour, J., de Gramont, X., 1986. Geological map of Fanjah, sheet NF 40-3F, scale:
691 1:100,000, with Explanatory notes: Directorate General of Minerals, Oman Ministry of
692 Petroleum and Minerals.
693 Whitehouse, M.J., Pease, V., Al-Khirbash, S., 2016. Neoproterozoic crustal growth at the margin
694 of the East Gondwana continent – age and isotopic constraints from the easternmost inliers
695 of Oman. International Geology Review 58, 2046-2064, doi:
696 10.1080/00206814.2016.1207207.